Vol. 7 № 3 Trans. Nonferrous Met. Soc. China Sep. 1997

LAMELLAR STRUCTURE IN LONG RANGE ORDERED PHASE δ'-$TiN_{0.5}$ ①

Yang Gaiying, Du Jun, Shi Likai
General Research Institute for Non-ferrous Metals, Beijing 100088

ABSTRACT Lamellar structure in long-range ordered δ'-$TiN_{0.5}$ phase was analyzed by transmission electron microscopy (TEM), and the crystallographic properties of the lamellar structure were discussed in terms of the crystal symmetry changes before and after transformation. It was shown that the lamellar structure is formed, at least locally, by plate pairs of any two of the three equivalent orientation variants. The interfaces between domain plates are always parallel to $\{011\}_M$ planes of the matrix, but there are only two possible equivalent orientations for any domain pair. During ordering transformation, the transformed products grow along the normal directions of the plates by way of combination of the two plates which form a domain pair, and this gives rise to the final lamellar structure in δ'-$TiN_{0.5}$ phase. Such lamellar structure may considerably reduce the elastic energy accumulated in the matrix around the precipitates during transformation.

Key words lamellar structure δ'-$TiN_{0.5}$ long-range ordering transformation

1 INTRODUCTION

In the framework of the disordered face centered cubic (fcc) δ-$TiN_{0.5}$ (space group: $Fm3m$), the titanium atoms in the apexes and the face centers form a close-packed fcc metallic sublattice with nitrogen atoms in the centers of the octahedral sites. If these octahedral sites are not all occupied, the unoccupied sites can be considered "vacancies" in the metalloid sublattice. The disordered δ-TiN_x phase exhibits a large nonstoichiometry with x varying from 0.38 to 1.10[1]. The lattice parameter a increases linearly with nitrogen content[2]. When isothermally annealed below 800 ℃, the δ-TiN_x phase of a composition in the vicinity of stoichiometry ($x = 0.50$) will undergo an ordering transformation: δ-$TiN_x \rightarrow \delta'$-$TiN_x$. The ordered δ'-TiN_x phase presents a tetragonal structure ($a = 0.4140$ nm, $c = 0.8805$ nm) with space group $I4_1/amd$[3].

The present study was undertaken to characterize and understand the lamellar structure found in ordered δ'-$TiN_{0.5}$ phase after ordering transformation. Such plate-shaped precipitates are quite similar to those of martensitic transformation products[4], and are also consistent with many other cubic-tetragonal phase transformations[5].

2 EXPERIMENTAL MATERIALS AND PROCEDURE

Based on Joule effects, the disordered δ-$TiN_{0.5}$ parent phase was obtained by direct nitridation of titanium plate[6]: A titanium plate with a purity higher than 99.99% was mounted between two Ti electrodes in a cold reactor and heated in ultra high vacuum (10^{-5} Pa) to 1 440 ±10 ℃, and then a proper amount of nitrogen gas was introduced to the cold reactor to give a composition of 34.7% (mole fraction) N in δ-TiN_x. After nitridation, the plate was homogenized at 1 375 ±10 ℃ for about 500 h. The ordering transformations were carried out under the following vacuum annealing conditions: pressure 10^{-5} Pa, temperature below 750 ℃. The TEM observations were performed with an JEOL-2000FX electron microscope operating at 200 kV.

---

① Received Jul. 28, 1996; accepted Oct. 14, 1996

3 EXPERIMENTAL RESULTS

With respect to the δ-$TiN_{0.5}$ fcc crystal lattice, there exist three equivalent orientation variants for the tetragonal δ'-$TiN_{0.5}$ phase[7]. To facilitate the analyses in the following sections, the definition of the three equivalent orientation variants and their orientation relationships with parent matrix were grouped into Table 1.

Table 1 Definition of equivalent orientation variants in δ'-$TiN_{0.5}$ phase and their orientation relationships with δ-$TiN_{0.5}$

p1	p2	p3
$[100]_\delta // [100]_{\delta'}$	$[100]_\delta // [010]_{\delta'}$	$[100]_\delta // [001]_{\delta'}$
$[010]_\delta // [010]_{\delta'}$	$[010]_\delta // [001]_{\delta'}$	$[010]_\delta // [100]_{\delta'}$
$[001]_\delta // [001]_{\delta'}$	$[001]_\delta // [100]_{\delta'}$	$[001]_\delta // [010]_{\delta'}$

The parent disordered δ-$TiN_{0.5}$ phase, when annealed at 600 ℃ for 2 h, begins to transform into the ordered δ'-$TiN_{0.5}$ phase. Fig. 1 shows the morphology and distribution of small nuclei of δ'-$TiN_{0.5}$ that is characteristic for the very early stage. The incident electron beam is parallel to $[\bar{1}32]_M$ direction of the matrix (Here the subscript M is referred to fcc coordinate system of the parent phase). Fig. 1(a) is a bright field image, and Fig. 1(b) is a dark field image obtained by using the superlattice reflection $\bar{1}01_{p1}$ of p1 type orientation domains (cf the inset SAD pattern in Fig. 1(a)). As a whole, the nucleation process of δ'-$TiN_{0.5}$ proceeds quite homogeneously in parent phase. At this first stage the size of the small precipitates is between 200 and 300 nm. It is clearly visible on the dark field image that the new phase is formed consisting of a number of parallel platelets or small domains, which are grouped together and elongated along some particular crystallographic directions. In the case of foil plane parallel to $[\bar{1}32]_M$ direction, the observed traces lie respectively in $[111]_M$, $[\bar{1}12]_M$, $[\bar{3}13]_M$ and $[\bar{5}11]_M$ directions (Fig. 1(b)).

Fig. 1 Morphology of nuclei of δ'-$TiN_{0.5}$ at very first stage of transformation (600 ℃, 2 h)

(a) —Bright field image;

(b) —Dark field image taken with $g = \bar{1}01p1$ superlattice reflection

Because of the parameter difference between the two phases ($\rho = (c(\delta') - 2c(\delta))/(2c_\delta) = 4.5\%$), the coherent precipitation of the δ'-$TiN_{0.5}$ will produce a strong and complex strain field in the vicinity of the new phase, which makes it difficult to clarify the microstructural features of the transformation when the nuclei are too small. With a prolonged annealing time under the similar thermal treatment, the δ'-$TiN_{0.5}$ precipitates grow to a size large enough for microstructural elucidation. Fig. 2 gives a dark field image micrograph showing the morphology of new δ'-$TiN_{0.5}$ in a sample subjected to an annealing of 5 h. The corresponding electron diffraction pattern was also embedded in the figure. The incident electron beam is parallel to $[100]_M$ direction of the matrix. This dark field image was formed using the 011_{p1} superlattice reflection of p1 orientation variant, thus making excited only p1 type domains. The bright precipitates are of lamellar structure which are elongated generally to certain crystallographic directions. These directions may be recognized as $[011]_M$, $[010]_M$ and $[01\bar{1}]_M$ in the framework of $\delta\text{-TiN}_{0.5}$ phase for this $[100]_M$ foil orientation.

Fig. 2 **Dark field image ($g = 011_{p1}$) showing morphology of new $\delta'\text{-TiN}_{0.5}$ in sample subjected to annealing for 5 h**

During analyses of $\delta\text{-TiN}_{0.5} \rightarrow \delta'\text{-TiN}_{0.5}$ ordering transformation, it was found that the ordered $\delta'\text{-TiN}_{0.5}$ phase is always formed in form of lamella. We will deal with the determination of these special planes in $\delta\text{-TiN}_{0.5} \rightarrow \delta'\text{-TiN}_{0.5}$ ordering transformation, taking p1 orientation domains as example.

In $[100]_M$ crystal orientation, three favorable growing directions are indicated by arrows in Fig. 2. The intersection lines of $(01\bar{1})_M$ and $(011)_M$ planes with the observation plane are parallel to $[011]_M$ and $[01\bar{1}]_M$ directions, this implies that the lamellae growing along $[011]_M$ lie on the $(01\bar{1})_M$ plane, whereas the lamellae growing in $[01\bar{1}]_M$ direction lie on $(011)_M$ plane. Similarly, $[010]_M$ direction is parallel to the intersection between the observation plane (100) and $(101)_M$ or $(10\bar{1})_M$ planes, therefore the lamellae growing in the $[010]_M$ direction were precipitated on the $(101)_M$ or $(10\bar{1})_M$ planes, which are inclined to an angle of 45° with respect to the observation plane.

Fig. 3 shows a typical morphology in fully transformed $\delta'\text{-TiN}_{0.5}$ (annealed at 750 ℃ for 6 h). Fig. 3(a) is a bright field image, Fig. 3(b) is the simulated corresponding diffraction pattern, Figs. 3(c) and 3(d) are dark field images taken with 101_{p1} and $01\bar{1}_{p2}$ superlattice reflections. By comparison of the bright and dark field images, it is concluded that the areas which are not excited in the dark field images are domains of p3 variant. These electron micrographs clearly show the characteristics of the lamellar structure in $\delta'\text{-TiN}_{0.5}$ ordered phase: blocks of plates formed by p_ip_j domain pairs. Each block has nucleated independently and has been

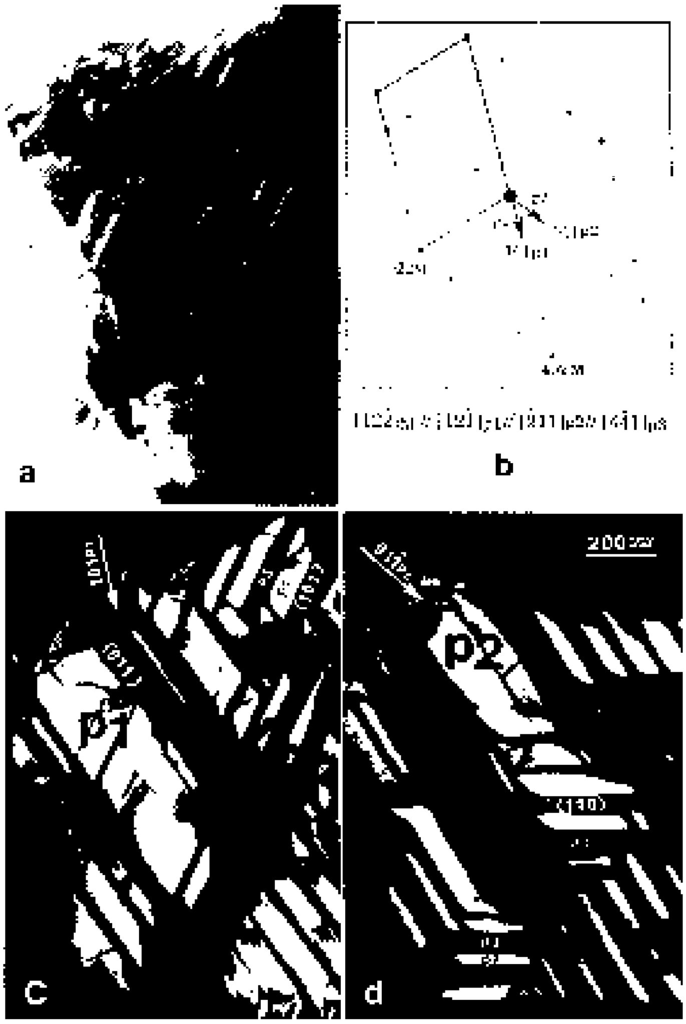

Fig. 3 **Typical lamellar structure in fully transformed $\delta'\text{-TiN}_{0.5}$ (annealed at 750 ℃ for 6 h)**

(a) —Bright field image; (b) —Simulated electron diffraction pattern along $[12\bar{2}]$; (c) and (d) —Dark field images taken with 011_{p1} and 101_{p2} superlattice reflections, respectively brought into contact by growth during further transformation. It is noted that the plate blocks have always the same types of interface for the same domain pairs: interface of p1p2 pair is $(011)_M$, interface of p2p3 pair is $(110)_M$ and interface of p1p3 is $(101)_M$. Also, can it be seen approximately that the three orientation variants have nearly the same volume fraction, indicating their crystallographic equivalence.

4 DISCUSSION

4.1 Interfaces between orientation domains

Experimental observations indicated that the interfaces between any orientation domain pair forming lamellar structure are always of the parallelism with $\{011\}_M$ of the matrix phase. The morphology of an inclusion depends on the number of equivalent variants, which in turn depends on the lattice orientation relationship and crystal symmetry changes before and after transformation.

Table 2 Crystallographic features of δ- and δ'-TiN$_{0.5}$

Phase	Space group	Point group	Lattice	Parameter / nm
δ	$Fm3m$ (a, b, c)	$\mid m3m \mid = 48$	$a = 0.4215$	–
δ'	$I4_1/amd$ $(a, b, 2c)$	$\mid 4/mmm \mid$ $= 16$	$a = 0.4140$	$c = 0.8805$

To illustrate this interrelationship, consider first the point group of invariance of δ/δ' (p1) bicrystal which represents a heterophase material. The point groups of the matrix δ and precipitates δ' (p1) are $Fm3m(a, b, c)$ and $I4_1/amd\ (a, b, 2c)$, respectively (Table 2). Given their relative orientation of the two phases (Table 1), the point group of the bicrystal $G\delta/\delta'$ (p1) is composed of the common operations to the point groups of the two phases, or $G\delta/\delta'$ (p1) is the intersection of them:

$$\begin{aligned} G\delta/\delta'(\mathrm{p1}) &= G\delta \cap G\delta'(\mathrm{p1}) \\ &= m3m(a, b, c) \cap \\ &\quad 4/mmm(a, b, 2c) \\ &= 4/mmm(a, b, 2c) \end{aligned}$$

Find out then all the equivalent orientations for a particular lamella in the matrix. Take one single orientation domain of p1 variant as an example. It is seen from the above section that the p1 variant may develop in the matrix in form of lamella with its extended face parallel to $(011)_M$ plane, expressed as p1$(011)_M$. With this configuration, the point group of invariance associated to the δ'-p1$(011)_M$ plate is composed of the elements in $G\delta'$ which make the plate strictly invariant (its normal may turn upside down), we have

$$G\delta'\text{-p1}(011)_M = 2/m[100]_M$$

Since $G\delta'$-p1$(011)_M$ is a subgroup of $G\delta/\delta'$ (p1), the number of p1 domain plates crystallographically equivalent to p1$(011)_M$ is given by the index of the subgroup in the group. There are 16 and 4 operating elements in $G\delta/\delta'$ (p1) and $G\delta'$-p1$(011)_M$, respectively, thus

$$\begin{aligned} N\delta'\text{-p1}(011)_M &= i\left(\frac{G\delta/\delta'(\mathrm{p1})}{G\delta' - \mathrm{p1}(011)_M}\right) \\ &= \frac{\mid 4/mmm(a, b, 2c) \mid}{\mid 2/m[100]_M \mid} \\ &= 16/4 = 4 \end{aligned}$$

This implies that there are 4 equivalent domain plates of p1 type. In other words, during the $\delta \to \delta'$-TiN$_{0.5}$ ordering transformation, the plates of p1 type can extend only on four planes among the six of $\{011\}_M$ family of the fcc matrix phase. Similarly, the domain plates for p2 and p3 variants exhibit also 4 equivalents. All the possible extended planes for the three orientation variants are grouped in Table 3.

Table 3 Possible extended planes of orientation variants in δ'-TiN$_{0.5}$

Orientation variant	Extended planes			
p1	$(011)_M$	$(01\bar{1})_M$	$(101)_M$	$(10\bar{1})_M$
p2	$(011)_M$	$(01\bar{1})_M$	$(110)_M$	$(1\bar{1}0)_M$
p3	$(101)_M$	$(10\bar{1})_M$	$(110)_M$	$(1\bar{1}0)_M$

It is evident that, among all the possible domain plates listed in Table 3, only those with a common extended plane as their interface might form a plate pair, which eventually results in lamellar structure in δ'-TiN$_{0.5}$ phase. For p1 and p2 variants, for example, their common extended planes are $(011)_M$ and $(01\bar{1})_M$. This means that the interface between p1 and p2 domain plates could only be either $(011)_M$ or $(01\bar{1})_M$, and there are only two possible crystallographically equivalent p1p2 plate pairs. Similar analytical conclusions follow for all domain plate pairs formed by any two of the p1, p2 and p3 variants and the results are grouped in Table 4.

Table 4 Equivalent orientations for domain plate pairs formed by p1, p2 and p3 variants

Pair	p1p2		p1p3		p2p3	
Interface	$(011)_M$	$(01\bar{1})_M$	$(101)_M$	$(10\bar{1})_M$	$(110)_M$	$(1\bar{1}0)_M$

The above analytical results can be confirmed by the electron micrographs in Fig. 4.

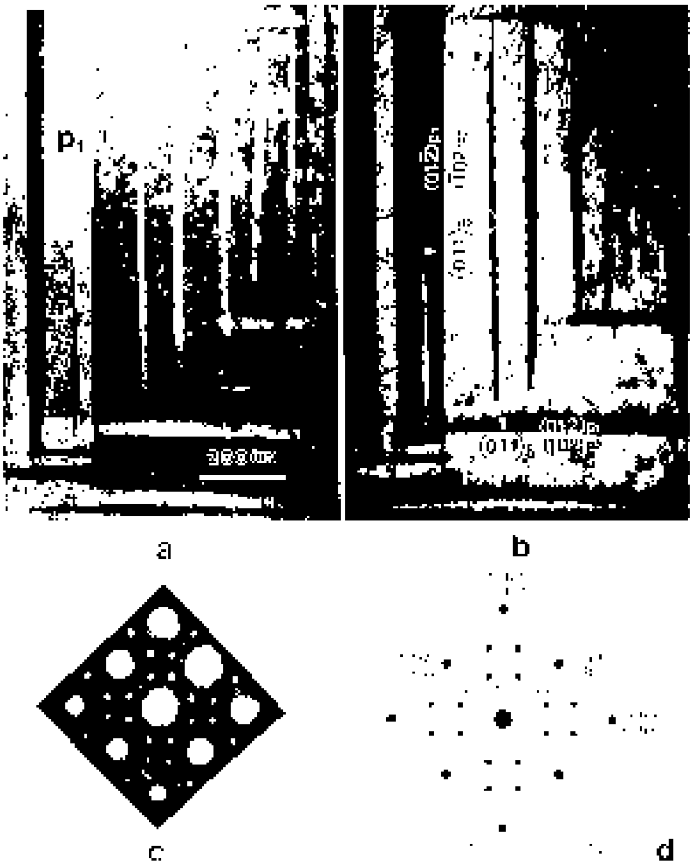

Fig. 4 Transmission electron micrographs showing two possible equivalent orientations $(011)_M$ and $(01\bar{1})_M$ for p1p2 orientation domain pair

(a) —Dark field image taken with (011) p1 superlattice reflection;

(b) —Dark field image taken with (101) p1 superlattice reflection

Fig. 4(a) and 4(b) are the dark field images, respectively, with (011) p1 and (101) p2 superlattice reflections along $[100]_M$ direction. In this observation region, two blocks of lamellar structure with the two possible extended planes between plates of p1 and p2 variants could be qualified.

In summary, each plane of the fcc $\{011\}_M$ family corresponds to one particular plate pair by parallelism to their extended faces which in turn exhibits two equivalent orientations among them. In addition, the analytical results compiled in Table 4 are useful for the elucidation of the TEM experimental results: for a given reference coordinate system, if the habit plane of a plate pair is qualified, the type of the plate pair will be known immediately.

4.2 Self-accommodating growth

If the two possible interfaces for any plate pair (p_ip_j) are exactly equivalent from the point of view of crystallography and thus have the same probability of existence, the three orientation variants p1, p2 and p3 tend, at least locally, to form plate-shaped blocks which are formed by only one of the equivalent orientations of the pair (i. e. $p_ip_jp_i$).

In fact, the orientation variants p1, p2 and p3 are strictly equiprobable in the cubic matrix, a very small enclosed particle of the new phase, however, should have to accommodate itself to the matrix and thus generally be elastically constrained into full coherence with the matrix. Because of the parameter differences between δ- and δ′-TiN$_{0.5}$ (a and b decrease: $0.4215\ \text{nm} \rightarrow 0.4140\ \text{nm}$, c increases: $0.4215\ \text{nm} \rightarrow \frac{0.8805}{2}$ nm), the strain field in the surrounding matrix is quite appreciable, which reduces its symmetry and thus makes to some extent the three variants inequivalent. This is well illustrated schematically by a single small plate-shaped precipitate of p1 variant shown in Fig. 5. The surrounding matrix of the plate is compressed in c direction and is extended in a, b directions. The crystal symmetry has been reduced from $m3m$ to $4/mmm$ in the region labeled A and the number of the equivalent orientation variants is now equal to

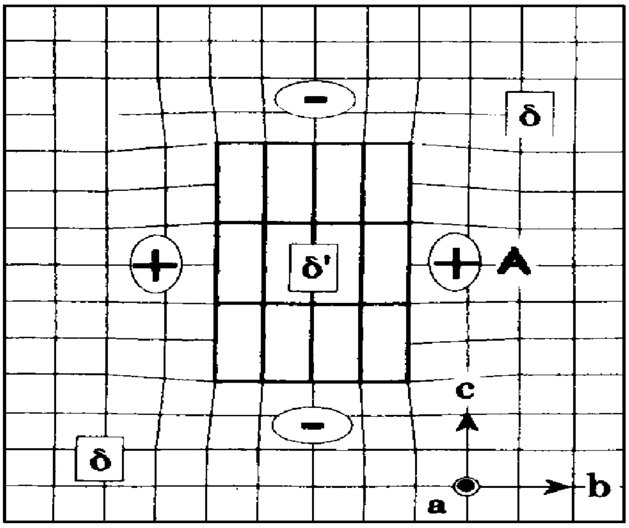

Fig. 5 Schematic representation of lattice deformation in surrounding matrix of a small p1 plate

$\frac{|4/mmm|}{|4/mmm|} = 1$. When a new nucleus of p2 variant forms in such deformed region, it will be invariant by application of the symmetry of the deformed matrix and p3 variant will not be engendered, and the plate-shaped pair will be p1p2. This implies that in a region of lamellar structure dominated by p1p2 pair, it is impossible for p3 variant to accommodate with p1p2 pair. If now a nucleus of p3 variant appears first, p3 variant will be crystallographically invariant, p2 variant will not be engendered, the plate pair will be p1p3.

An enclosed particle of the new phase, in or near equilibrium, has a preferred morphology that is mainly determined by the additional free energy which consists of the interfacial free energy and elastic strain energy in the surrounding matrix. At the first stage of the ordering transformation, the new nuclei precipitate homogeneously in the matrix (Fig. 1). During further growing, however, the strain energy will become increasingly important because this energy is proportional to the volume of the precipitate, which makes it very difficult for a plate-shaped orientation domain to grow along its normal direction. If a new p2 type plate is formed upon an existing p1 type plate, the elastic fields in the matrix induced by the two variants will have opposite signs and their effects will be largely cancelled (Fig. 6), leading to a substantial decrease in the overall free energy. And then another new p1 plate forms upon the p2 plate …(since p1p2 is, locally, a crystallographical invariant), the transformation can thus proceed along the normal direction. In this way, the final lamellar structure of δ' is obtained as shown in Fig. 7 (a), and the elastic strain field in the surrounding matrix exhibits a typical zigzag form (Fig. 7 (b)). It is obvious from Fig. 7(b), that the amplitude of the strain energy is a function of the

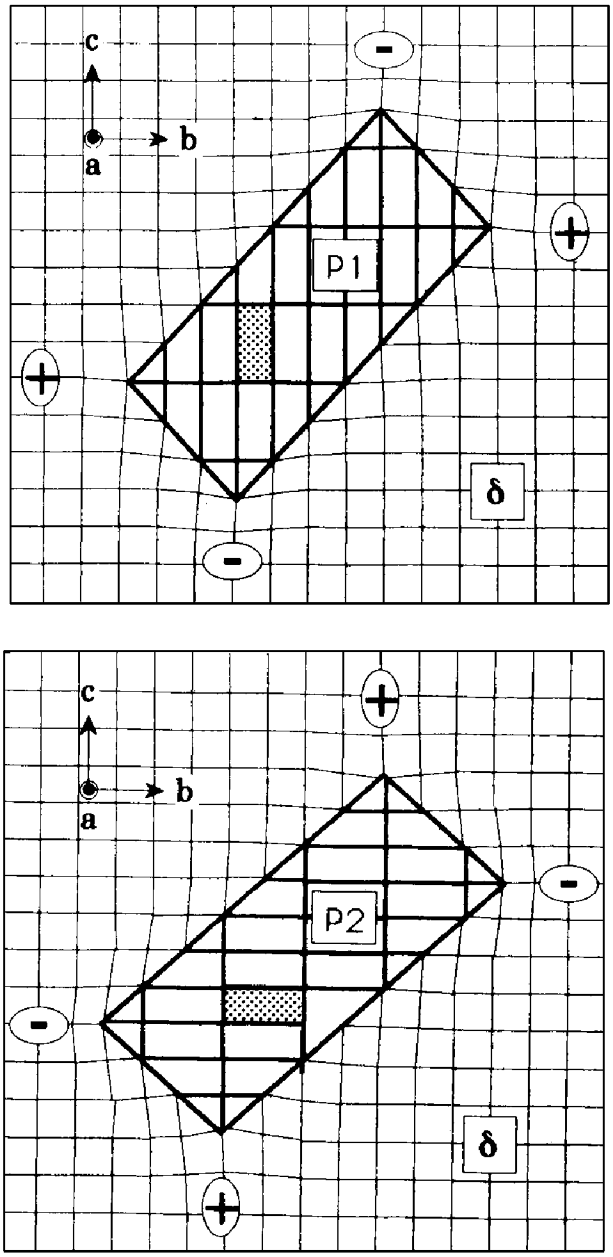

Fig. 6 Opposite signs of deformation in matrix lattice caused by p1 and p2 plates

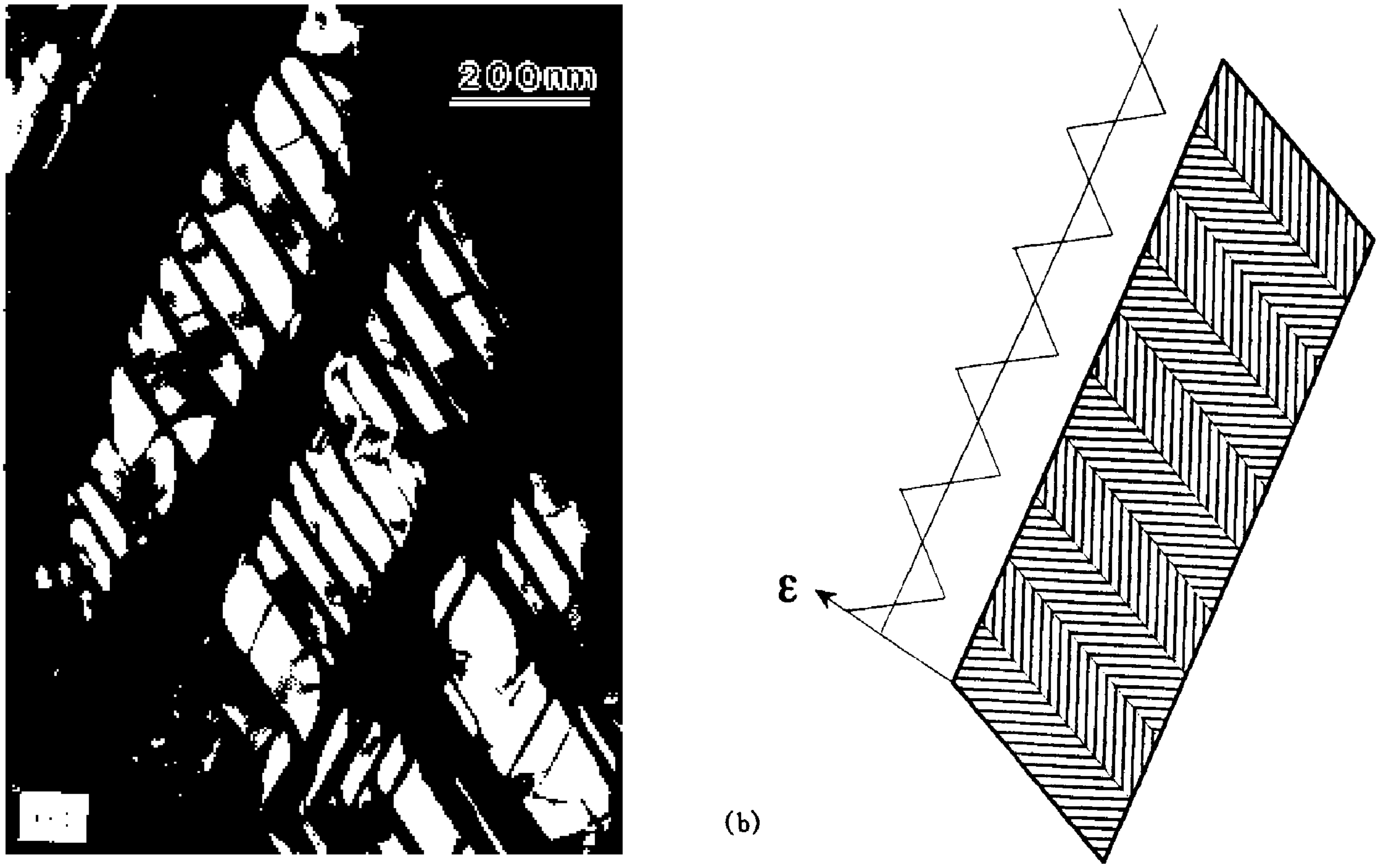

Fig. 7 Orientation domain plates of p1p2 pair (a) and schematic appearance of deformation strain in matrix surrounding them (b)

thickness of the plates which is determined by the resistance of the matrix to the elastic deformation and the interfacial free energy. The smaller the thickness is, the smaller the strain energy will be. While this kind of lamellar structure has also been observed in some other cubic→tetragonal transformations, its formation mechanism for reducing the strain energy is really quite similar to that in plate-shaped martensitic transformation microtwins[4].

5 CONCLUSIONS

(1) Long-range ordered $\delta'\text{-TiN}_{0.5}$ domain plates are always extended upon $\{011\}_M$ planes of the $\delta\text{-TiN}_{0.5}$ parent phase.

(2) Interfaces of all domain pairs are also parallel to the planes of $\{011\}_M$ type; however, for a particular domain pair, only two among the six planes of $\{011\}_M$ could be their interfaces.

(3) Lamellar structure in $\delta'\text{-TiN}_{0.5}$ is formed by pairs of the three equivalent orientation domains by way of self-accommodating growth along the normal direction of the plates, which is due to the relaxation of the strain energy accumulated in the surrounding matrix of the plates during nucleation and growth processes.

REFERENCES

1 Gusev A I. Phys Stat Sol (b), 1985, 163: 17.
2 Xriedt H, Murry J L. Bull Alloy Phase Diagr, 1987, 8: 378.
3 Lobier G, Marcon J P. Cr Acad Sci Paris, 1977, 10: 52.
4 Wayman C M. Metall Mater Trans A, 1994, 25: 1787.
5 Khachaturyan A G. Theory of Structural Transformations in Solids. New York: John Wiley & Sons, 1986: 368- 407.
6 Etchessarhar E. J Less Com Met, 1991, 167: 261.
7 Yang G Y, Du J, Portier R, Shi L K. The Chinese Journal of Nonferrous Metals, (in Chinese), 1994, 4 (suppl): 143.

(Edited by Peng Chaoqun)